Arabian Journal for Science and Engineering (2023) 48:3441–3454
https://doi.org/10.1007/s13369-022-07162-0

RESEARCH ARTICLE-MECHANICAL ENGINEERING

Influence of Water Mist Nozzle Characteristic Parameters on Oil Pool Fire Extinguishing in Confined Space

Xiaohong Gui[1] · Haiteng Xue[1] · Zhengyu Hu[1] · Zehui Cui[1]

Received: 19 March 2022 / Accepted: 21 July 2022 / Published online: 16 August 2022

Abstract
In order to explore the effect of characteristic parameters of water mist nozzle on oil pool fire in confined space, mathematical model and physical model of oil pool fire in confined space were established. The effects of nozzle characteristic parameters such as water mist atomization cone angle, spray speed, droplet size and spray flow on fire extinguishing in a naturally ventilated room were discussed by using large eddy method and Lagrange method. The research illustrates that when atomization cone angle is in a certain range (80°–110°), fire extinguishing time is gradually shortened, and cooling effect of water mist is improved with the increase of atomization cone angle. When spray speed is 5–20 m/s, the greater the spray speed, the better the cooling effect. When droplet size is 100–300 μm, there is a positive correlation between droplet size and fire cooling rate. When the droplet size is greater than 300 μm, there is a negative correlation between droplet size and fire cooling rate. The inhibition of water mist on heat release rate increases with the increase of droplet size. The water mist with small particle size has a good cooling effect on the ceiling because of its overflow effect. In a naturally ventilated room, the water mist with the droplet size of 300 μm has a good cooling effect on the oil surface, and the reasonable droplet size is 300 μm. When the spray flow is 10–20 L/min, the greater the spray flow, the better the extinguishing effect.

Keywords Water mist · Confined space · Oil pool fire · Numerical simulation · Parameter optimization

1 Introduction

The frequent occurrence of oil pool fires in the process of use, transportation and storage has caused huge economic losses and environmental pollution. However, most fires occur in confined spaces with natural ventilation. Due to confined space, the fire will spread rapidly and then threaten the life safety of personnel, causing heavy casualties. Therefore, the prevention and control of indoor fire are always in an important position in the development of human society.

At present, the research on water mist fire extinguishing has been quite extensive. Yang et al. [1] used a single liquid nozzle with a maximum working pressure of 0.8 MPa to generate water mist and applied it to methyl methacrylate fire. The extinction of water mist is a combination of flame and fuel surface cooling, based on oxygen asphyxiation and thermal radiation. Gupta et al. [2] simulated the heptane pool fire in the combustion chamber. It is concluded that the maximum fire extinguishing speed is in the center of the spray symmetric combustion chamber. Yang et al. [3] studied the relationship between oxygen concentration and flame temperature by changing flame size, the number of nozzles, system working pressure and combustion time in closed combustion chamber. Paolo et al. [4] experimented with the burning of wooden crib. The effects of spray pressure, nozzle diameter, water mist flow and initial spray pulse were changed, and the suppression effect of water mist on solid flame was experimentally obtained. Arvidson et al. [5] conducted a fire test of large cargo transport vehicles on the tank deck and compared the fire extinguishing effects of high-pressure water mist fire extinguishing system and traditional water mist fire extinguishing system. Li et al. [6] changed the working pressure of the nozzle to produce different water mist curtains and studied the attenuation effect of fire and thermal radiation in a large diesel pool. Schmidt et al. [7] discussed the behavior of a single droplet ejected from the nozzle in the hot air environment caused by indoor fire and established a semi-empirical model based on the conservation of mass, momentum and energy to evaluate the heat and

✉ Xiaohong Gui
gxhbox@sina.com

[1] China University of Mining and Technology (Beijing), Beijing 100083, China

mass transfer phenomenon in the air water droplet system. Vouros et al. [8] realized the influence of heat flow on water mist light by using a horizontal heating plate. The research shows that the heat flow in the plate affects the development of light beam, reduces turbulence and has a significant impact on the volume flow of droplets. Santangelo et al. [9] compared the control effect and fire extinguishing effect of sprinkler system and water mist fire extinguishing system in closed parking lot fire based on experiments and compared the fire spread and fire control effect of the two fire extinguishing systems through the temperature measurement of the two fire extinguishing systems. The research shows that the water mist fire extinguishing system has a better fire extinguishing effect. Wang et al. [10] studied the protective effect of water mist curtain on glass and proved that water mist curtain could effectively protect glass from damage. Du et al. [11] established the nozzle flow field model, carried out comparative simulation analysis and analyzed the influence of nozzle diameter and nozzle distance on atomization performance. It is concluded that the suppression effect of the optimized nozzle on fire temperature is better than that of ordinary nozzle. According to the conclusion of Wyl's test [12], when there is finer smoke in the early stage of fire, it is effective to suppress the fine smoke without water mist.

In terms of oil pool fire extinguishing, Lin et al. [13] studied the effects of different pool sizes and regression rates on the flame height and entrainment of oil pool fire under static air and cross-flow conditions. The results show that when the inclination of the nearby surface is 0°, 20°, 30° and 40°, from the horizontal direction, the cross-flow velocity is 0–3 m/s, and the flame height increases with the increase of the inclination of the nearby surface. Zhao et al. [14] conducted fine large eddy simulation on a typical methanol pool fire structure with a diameter of 30 cm to evaluate the ability of current fire models to predict flame structure and liquid fuel surface heat transfer rate. Zhao et al. [14] conducted a fine large eddy simulation on a typical methanol pool fire structure with a diameter of 30 cm to evaluate the ability of current fire models to predict the flame structure and liquid fuel surface heat transfer rate. Wu et al. [15] simulated transformer oil fire with steel oil tank and discussed the combustion characteristics of large oil pool fire. The results show that with the increase of vertical height, the temperature near the tank wall decreases, and the growth rate of flame height increases with the increase of initial fuel temperature. Ji et al. [16] conducted experimental research on the flame radiation characteristics of oil pool fire, including flame emissivity, diameter and temperature. The flame height, mass loss rate, temperature distribution, flame emissivity and radiant heat flux were measured. Tian et al. [17] studied the change law of methanol pool fire combustion rate under the conditions of natural ventilation and mechanical ventilation through experiments. The heat transfer mechanism of methanol pool fire was deeply analyzed by changing the size of the plate, the initial temperature of the plate and the air velocity. Chen et al. [18] conducted an experimental study on the flame characteristics and temperature distribution of single kerosene pool and multi-kerosene pool fires under the action of crosswind through 13 test cases and fuel discs with different diameters and shapes. The study shows that there are three stages in the flame evolution process: preheating, stable combustion and extinction. Kong et al. [19] designed a small oil pool open water fire experimental system. The effects of oil pool diameter, oil layer thickness and wind speed on flame length and flame inclination were studied through experiments. The flame characteristics and temperature of the combustion system were recorded. It is concluded that the combustion behavior evolves from short pool fire to long attenuation stage and passes through the boiling stage. Gelderen et al. [20] studied the thermal properties and combustion efficiency of fresh crude oil, weathered crude oil and refined fuel oil to improve the available input data of the on-site ignition system for crude oil combustion. The results show that increasing the thermal feedback to the fuel surface is not the only factor to improve the combustion efficiency of a large-scale fire. Joe et al. [21] used a cone calorimeter to study the effect of radiant heat flux on the ignition and combustion behavior of typical oil products (diesel, lubricating oil and aviation kerosene). The ignition time, heat release rate, mass loss rate, extinction coefficient, CO and CO_2 yields were calculated by the standard oxygen consumption method. It is found that heat release rate, mass loss rate and CO/CO_2 ratio are positively correlated with radiant heat flux.

Compared with the widely used halon fire extinguishing agent, the water mist fire extinguishing technology does not produce environmental pollution, is friendly to the atmospheric ozone layer, can extinguish the fire efficiently, has low water consumption, high economic benefits and basically does not cause secondary disaster losses to the protected objects. However, the water mist fire extinguishing system is a complex multivariable system, and the fire extinguishing mechanism is complex, so there is no clear understanding at present. On the one hand, the chemical and physical effects between the water mist and the plume formed by fire are very complex, and the mechanism of the fog field is difficult to be explored. On the other hand, there is no definite conclusion about the form and result of the interaction between water mist and fire. Relevant research has not found a quantitative method to evaluate the fire extinguishing effectiveness of water mist, which greatly limits the development and utilization of water mist system.

In order to explore the mechanism of pulsed water mist fire extinguishing and optimize nozzle parameters, the large eddy simulation method and Lagrange particle method are used to

simulate the action process of water mist extinguishing oil pool fire in confined space. By comparing the water mist fire extinguishing conditions of different spraying methods, the water mist fire extinguishing efficiency is comprehensively analyzed and the rules are summarized. The effects of spray cone angle, spray speed, droplet size and spray flow on confined space oil pool fire suppression are simulated. The optimal parameters are determined by analyzing and comparing the cooling, heat release rate and thermal radiation changes, in order to provide a reference for the parameter optimization of pulse water mist and nozzle design.

2 Numerical Simulation

2.1 Control Equation of Water Mist Extinguishing Oil Pool Fire in Confined Space

2.1.1 Conservation Equation [22]

Mass conservation equation:

$$\frac{\partial \rho}{\partial t} + \nabla \cdot \rho\mu = 0 \tag{1}$$

where ρ is density, kg m^{-3}; t is time, s; μ is flow rate, m s^{-1}.

Momentum conservation equation:

$$\frac{\partial(\rho\mu)}{\partial \mathrm{t}} + \nabla \cdot \rho\mu^2 + \nabla p = \rho f + \nabla \cdot \tau_{\mathrm{i}} \tag{2}$$

where p is pressure, Pa; f is buoyancy, N; τ is shear stress, Pa.

Component conservation equation:

$$\frac{\partial(\rho Y_i)}{\partial t} + \nabla \cdot \rho Y_i \mu + \nabla p = \rho D_i \nabla Y_i + m_i^{''} \tag{3}$$

where Y_{i} is concentration of component i, mol·L^{-1}; D_{i} is diffusion coefficient of component i, $m^2 \cdot s^{-1}$; $m_i^{''}$ is mass production rate of component i in the unit space.

2.1.2 Turbulence Model

The fire scene in the numerical simulation conforms to the turbulence model. In this paper, large eddy simulation is adopted. Due to its meshing characteristics, it is difficult to fully cover the mixing process in each relevant scale. Therefore, in the treatment of fluid viscosity, the sub-lattice stress scale model is used, which is set as an empirical constant in the model, and the dynamic viscosity coefficient of momentum equation is expressed as [22]:

$$\mu_{LES} = \rho(c_S\Delta)^2\left[2(defu)\cdot(defu) - 1.5(\nabla \cdot u)^2\right]^{0.5} \tag{4}$$

where *defu* is deformation rate of fluid micelles; c is empirical constant; Δ is length of cell mesh.

The large eddy simulation method is used to deal with turbulent flow. The purpose of large eddy simulation method is to select a filter width between the large-scale vortex structure and small-scale vortex structure (Kolmogorov scale) of the flow field to filter the control equation, so as to divide all variables into large-scale and small-scale quantities, directly simulate the large-scale quantities and directly calculate them by solving the differential equation of motion. The dissipation effect of small-scale quantities on large-scale energy is expressed as a stress term similar to Reynolds stress in the equation of motion. The sublattice stress model is used for simulation. The accuracy of large eddy simulation results is very high when the appropriate sublattice model is adopted. The above characteristics of large eddy simulation determine that the simulation result is a physically real transient flow field, which plays an important role in deeply understanding the essence of the flow field. By solving a set of Navier–Stokes equations (viscous fluid equations) describing thermally driven low-speed flow, the large eddy simulation method focuses on the calculation of smoke flow and heat transfer process in fire. The finite difference method is used to calculate the temperature and density of gas in the same three-dimensional flow, and the finite difference method is used to calculate the temperature and density of the gas in the finite volume. The growth and spread of fire are calculated in combination with the material characteristics of walls, floors, and ceilings in the confined space. After the simulation solution, a series of data such as temperature, CO concentration and visibility at relevant measurement points can be obtained.

2.1.3 Droplet Model

For the water mist opened in the fire simulation, the droplet size refers to the average diameter of the droplet volume, and 50% of the total volume of the water mist is located in this particle size. The droplet size follows the log-normal/Rosin–Rammler distribution [23].

Lagrange method is used to simulate the interaction between water mist and flame, and couple's discrete droplets with continuous gas phase through different forces. The main difference of liquid phase model lies in the described methods of a large number of water mist droplets, mainly including the Euler method and Lagrange method. In the former, the gas–liquid two phases pass through friction, heat and mass

Table 1 Thermal properties of materials

Material	Thermal conductivity $W\cdot(m\cdot K)^{-1}$	Heat capacity $J\cdot(kg\cdot K)^{-1}$	Density $kg\cdot m^{-3}$
Cement	1.6	750	2400
Steel	45.8	460	7850

Table 2 Model parameters

Model	Size
Computational model	2.2 m × 1.8 m × 2.5 m
Wall	0.5 m (Thickness)
Floor	0.5 m (Thickness)
Opening	2 m × 0.8 m

transfer, and the calculation depends on the volume fraction of each phase in the grid element. The latter considers the interaction through various interaction forces. The particle phase is regarded as a discrete particle group. Each physical quantity describing the dispersion of the particle group is solved in the Lagrange coordinate system, and the statistical method is used to statistically average the macrocharacteristics of the particles. **The** Euler method is more suitable for dense phase simulation. **The** Lagrange method is more suitable for sparse phase simulation, and the trajectory of particle dispersion can be clearly simulated, which has strong applicability. In this paper, the Lagrange method is used to simulate the interaction between hot flue gas and fine water droplets. The droplets are regarded as many independent small particles. The coupling between these discrete small droplets and continuous gas phase is realized by different forces. Due to **a** large number of droplets, the trajectory of each droplet cannot be tracked one by one. Generally, the motions of 1000 droplets are tracked every 1 s (also equivalent to tracking 50 droplets every 0.05 s) (Tables 1 and 2).

2.2 Physical Model

The simulated confined space is set as an indoor environment with a length of 2 m, a width of 1.8 m and a height of 2.5 m. The materials are steel and cement. A door is set on the right side with an opening size of 2 m × 0.8 m, in the state of natural ventilation. The wind speed at the center of the window is set to be about 1 m/s. The specific velocity is set to be 1.0 m/s. The calculation area is extended laterally to the right by 0.2 m to reduce the influence of the room opening air flow due to the boundary calculation area. The water mist device is set at a height of 2.4 m, and the fire source is placed 0.6 m away from the center of the room. The fuel is gasoline with a size of 0.3 m × 0.3 m × 0.3 m. The relevant parameters of gasoline are shown in Table 3. The ambient temperature is 25 °C. The upper part of the oil pool is divided into constant flame area ($0 < Z/Q^{0.4} \leq 0.08$), intermittent flame area ($0.08 < Z/Q^{0.4} \leq 0.2$) and buoyant plume area ($0.2 < Z/Q^{0.4}$) [23]. Thermocouple devices and gas detection devices are set at 20 cm, 115 cm and 150 cm above the oil pool, respectively. Longitudinal temperature, water vapor and oxygen concentration slices are set at the center of the fire source. The physical model and measuring point diagram are shown in Fig. 1. The thermal properties of materials are shown in Table 1. The model parameters and the physical parameters of gasoline are shown in Tables 2 and 3, respectively.

2.3 Meshing

By the comparison of numerical simulation results including four mesh sizes with 0.04 m × 0.04 m × 0.04 m (I), 0.05 m × 0.05 m × 0.05 m (II), 0.06 m × 0.06 m × 0.06 m (III) and 0.08 m × 0.08 m × 0.08 m (IV); the most appropriate grid size is selected. The power of the fire source is set at 1500 kW, and the thermocouple is set at 0.2 m away from the center of the fire source.

Figure 2 shows the temperature versus time within one minute after grid calculation of four different sizes. It can be seen from Fig. 2 that the operation results of grid (I) and grid (II) are very similar, and the temperature change curve is very close. The results of grid (III) are obviously different from those of grid (I) and grid (II), while the results of grid (IV) with the largest size are the most different from those of the other three grids. The calculation time of grid (II) is less than that of grid (I). It can also be seen from Fig. 3 that the smaller the grid element is, the more accurate the description of flame shape is, and the closer the flue gas distribution is to the actual combustion state. To sum up, 0.05 m × 0.05 m × 0.05 m is used as the grid far away from the fire source, and the grid division of the model is shown in Fig. 4.

3 Numerical Simulation Analysis of Water Mist Extinguishing Oil Pool Fire

Based on the large eddy simulation of turbulence, the mixed fraction model is used to simulate combustion reaction. The radiation property of hot flue gas adopts gray body radiation. The radiation property of fog droplets is calculated according to Mie theory (Mie light scattering theory). The flame extinction is controlled by the limiting oxygen index and critical flame temperature. The two-phase interaction between water mist particles and flame is described by Lagrange method, and the numerical model of the interaction between water mist and oil pool fire is established. The interaction between

Table 3 Physical parameters of gasoline

Relative molecular mass	Density ($kg \cdot m^{-3}$)	Specific heat capacity $kJ \cdot (kg \cdot K)^{-1}$	Thermal conductivity $W \cdot (m \cdot K)^{-1}$	Calorific value of combustion ($kJ \cdot kg^{-1}$)	Heat of vaporization ($kJ \cdot kg^{-1}$)
93	900	1.842	0.137	46,000	551

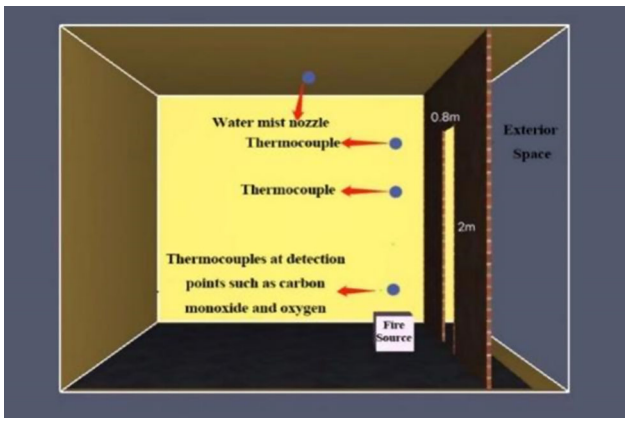

Fig. 1 Schematic diagram of model and measuring points

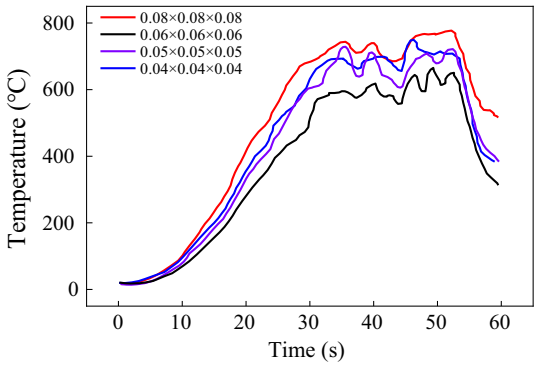

Fig. 2 Flame and flue gas shapes under grids of different sizes

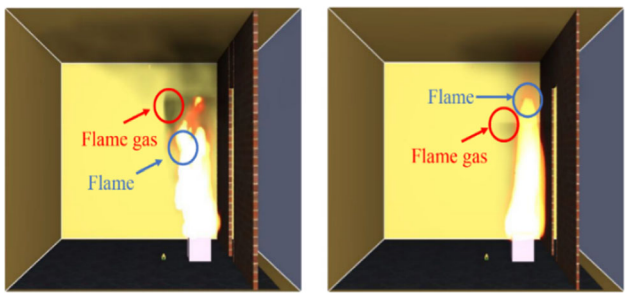

(a) Large grid **(b)** Small grid

Fig. 3 Flame and flue gas shapes under grids of different sizes. **a** Large grid. **b** Small grid

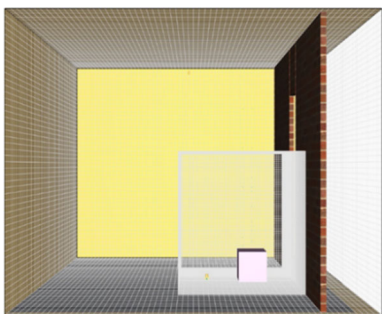

Fig. 4 Mesh generation of model

Table 4 Parameter settings of water mist nozzle

Water mist droplet size (μm)	Jet speed ($m \cdot s^{-1}$)	Flow ($L \cdot min^{-1}$)	Atomization cone angle (°)
300	7	10	50
300	7	10	60
300	7	10	70
300	7	10	80
300	7	10	95
300	7	10	110
300	7	10	120

water mist and gas diffusion flame is numerically studied by spray cone angle, spray speed, droplet size and spray flow. The calculation results show that for a given water mist fire extinguishing system, there is an optimal nozzle characteristic parameter, which can produce the highest penetration capacity.

3.1 Influence of Atomization Cone Angle on Fire Extinguishing

The atomization cone angle not only directly determines the distribution of droplets in space, but also affects the initial velocity and momentum of droplets. It is an important parameter affecting the fire extinguishing ability of droplets passing through obstacles [18]. In order to explore the influence of atomization cone angle on fire extinguishing effect in confined space, several different atomization cone angles of 50°, 60°, 70°, 80°, 95°, 105°, 110° and 120° are selected. Table 4 shows the parameters of water mist nozzle.

3.1.1 Oil Surface Temperature Analysis

The temperature changes of fuel surface temperature measuring points with time under five working conditions in the simulation are sorted out, and the cooling effect of the fire of the pulse water mist fire extinguishing system with different atomization cone angles is obtained, as shown in Fig. 5.

It can be seen from Fig. 5a that when the water mist cone angle is 50°, 60° and 70°, the maximum temperature of the fuel surface reaches 767 °C after full precombustion. When the water mist system is started in the 30 s, the fuel surface temperature drops rapidly by about 200 °C, and then the temperature of the measuring point fluctuates between 150 and 400 °C, and the simulation time is extended to 1000 s. The temperature still has no obvious downward trend and is in a stable combustion state. At the same time, the overall temperature curve with the atomization cone angle of 70° is lower than that of 60° and 50°, which is mainly because the cooling effect of the water mist system is enhanced with the increase of the atomization cone angle. Within this range, the temperature is controlled to a certain extent, but it is not enough to be extinguished.

Figure 5b shows that the fire can be extinguished successfully under the working conditions of 80°—120°. After sufficient precombustion, the maximum temperature reaches 767 °C, and the temperature drops rapidly after opening the water mist nozzle for 30 s. Among them, the temperature continues to drop to the room temperature when the atomization cone angle is 105°, 110° and 120°; it takes 55 s to drop to the safe temperature under the working condition of 105°, 42 s to drop to the safe temperature under the working condition of 110° and 42 s to drop to the safe temperature under the working condition of 120°. The temperature rises when it drops to about 200 °C under the working conditions of 80°–95°. The temperature reaches the second peak at about 44 s. The fire extinguishing time under the working condition of 80° is 92 s and that under the working condition of 95° is 91 s.

It can be seen from Table 5 that when the atomization cone angle is 80°–110°, with the increase of the atomization cone angle, the cooling effect of water mist gradually increases, and the fire extinguishing time gradually shortens. When the spray cone angle is greater than 110°, the extinguishing time is no longer significantly shortened. This is because the continuous expansion of the water mist spray range leads to the reduction of the unit effective mist flux, which is not conducive to improving the fire extinguishing efficiency, so the time will not continue to decrease. However, in terms of reducing to room temperature, the atomization cone angle of 120° is slightly shorter than that of 110°, because the fire source has been controlled at this time, and a wide range of water mist is conducive to the recovery of indoor air to room temperature. This shows that the increase of atomization cone angle can improve the fire extinguishing effect greatly, but it is limited. Therefore, the atomization cone angle with the best cooling effect in the fire scene should be 110°.

3.1.2 Analysis of Heat Release Rate and Thermal Radiation

After sorting out the changes of fuel heat release rate and thermal radiation with time under five working conditions in the simulation, the cooling effect of the fire of the pulse water mist fire extinguishing system is obtained when the atomization cone angle is different, as shown in Fig. 6.

It can be seen that after the water mist nozzle is turned on, the heat release rate decreases rapidly. When the atomization cone angle is 120°, 110°, 105°, 95° and 80°, the time to reduce the heat release rate to 0 kW is 49 s, 55 s, 59 s, 96 s and 106 s, respectively. Therefore, with the increase of atomization cone angle, the inhibition effect of water mist on heat release rate is gradually obvious.

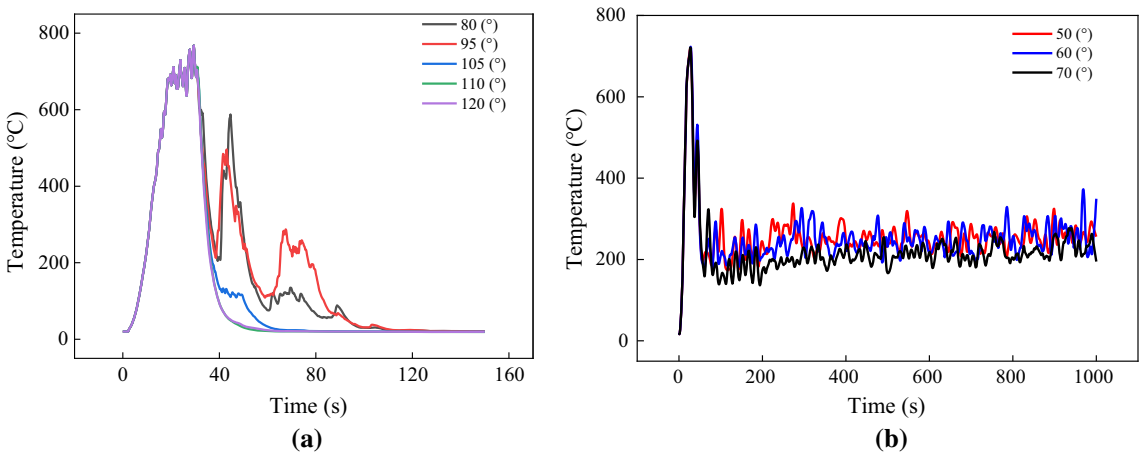

Fig. 5 Variation of temperature with time under different atomization cone angles

Table 5 Fire extinguishing time under different atomization cone angles

Atomization cone angle (°)	80	95	105	110	120
Time to safe temperature (s)	92	91	55	42	42
Time to room temperature (s)	109	106	63	57	54

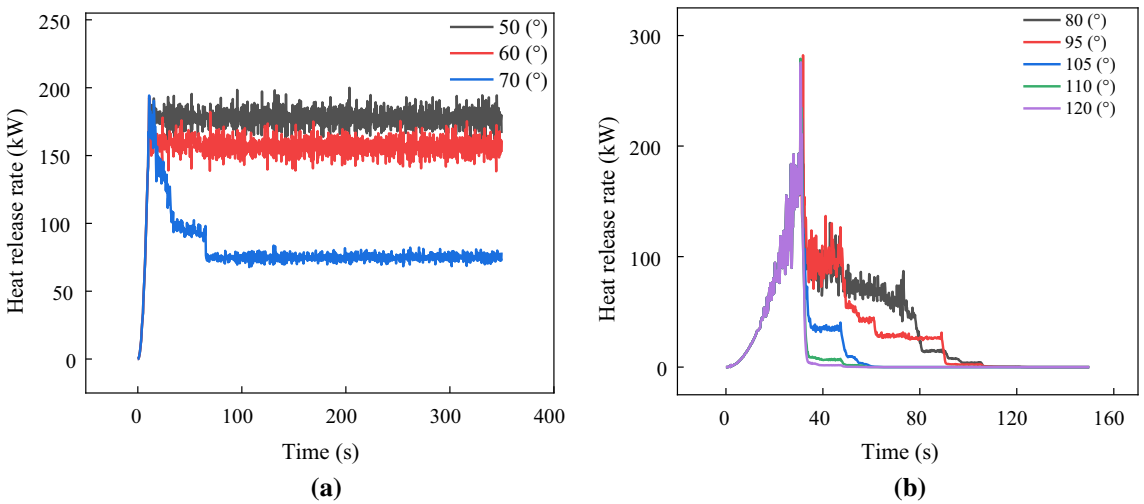

Fig. 6 The curve of heat release rate change

Therefore, the maximum value of heat release rate is also greater. When the atomization cone angle is 50°–70°, the maximum heat release rate is about 190 kW, while when the atomization cone angle is 80°–120°, the maximum heat release rate is close to 260 kW. This is because when water mist is applied, the flame will be in a relatively strong turbulent state, which will aggravate the combustion rate of fuel. The larger the atomization cone angle is, the larger the coverage of water mist is. The turbulence caused by the disturbance to the flame is also stronger, so the maximum value of heat release rate is also greater.

It can be seen from Fig. 7 that the variation trend of thermal radiation with time in the fire site is very similar to that of heat release rate with time. When the atomization cone angle is 105°, the thermal radiation is shielded in a wide range, fluctuates in the range of 18–40 kW and reduces to 0 kW at 400 s. When the atomization cone angle is 110°–120°, the shielding effect of thermal radiation is extremely close and reduces to 0 kW at about 240 s.

3.1.3 Water Mist Morphology Under Different Atomization Cone Angles

The atomization cone angle is expansion range of water mist with the nozzle as the origin. Water mist forms with atomization cone angles of 60° and 110° are shown in Figs. 8

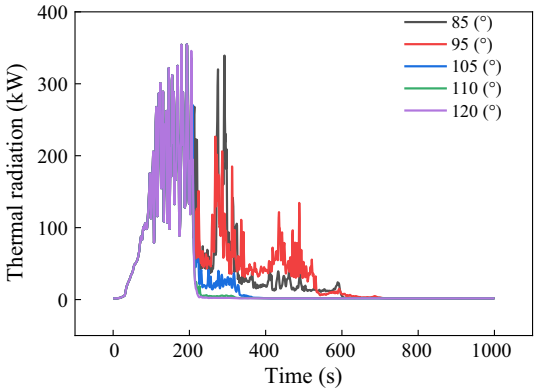

Fig. 7 The curve of thermal radiation change

and 9, respectively. It can be seen that the atomization cone angle directly affects the contact surface between water mist and combustibles, resulting in the speed of fire extinguishing process. When the atomization cone angle is small, for the fire source or obstacle fire that is not directly below the water mist, the water mist cannot contact the fire source.

In a large area, the fire extinguishing capacity is limited and even leads to fire extinguishing failure. When the atomization cone angle increases, the action range of water mist will also increase. When the atomization cone angle is 110°, the water vapor formed by the combined action of water mist and high temperature can cover the fire source to a large extent, and the fire extinguishing effect is good.

Table 6 Parameter settings of water mist nozzle

Water mist droplet size (μm)	Jet speed ($m \cdot s^{-1}$)	Flow ($L \cdot min^{-1}$)	Atomization cone angle (°)
300	5	10	110
300	10	10	110
300	20	10	110
300	30	10	110

3.2 Effect of Spray Speed on Fire Suppression

In order to investigate the influence of spray speed on fire extinguishing effect in confined space, four different spray velocities of 5 m/s, 10 m/s, 20 m/s and 30 m/s are selected for numerical simulation when other parameters remain unchanged. Table 6 shows the parameter settings of water mist nozzle.

3.2.1 Analysis of Oil Surface Temperature

After sorting out the temperature change of the temperature measuring points on the fuel surface with time under four working conditions in the simulation, the fire cooling effect of the pulse water mist fire extinguishing system is obtained when the spray speed is different, as shown in Table 7 and Fig. 10.

It can be seen from Fig. 10 that the increase of spray speed can improve the cooling and fire extinguishing effect

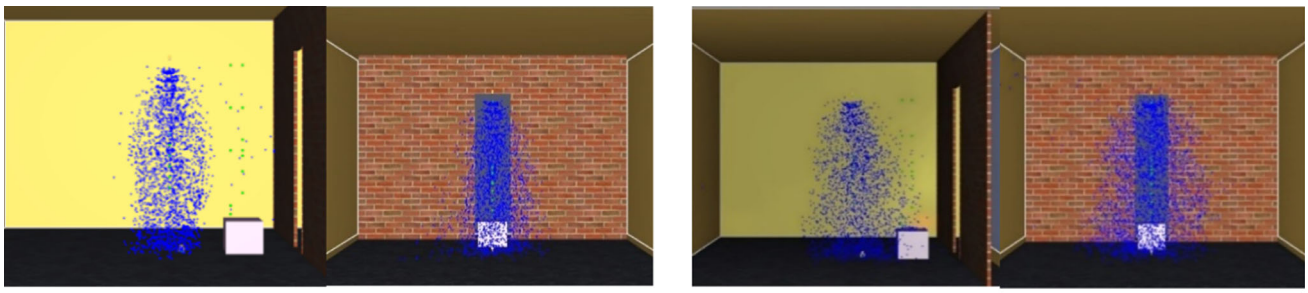

(a) Water mist morphology with atomization cone angle of 60°

(b) Water mist morphology with atomization cone angle of 110°

Fig. 8 Water mist distribution patterns with different atomization cone angles

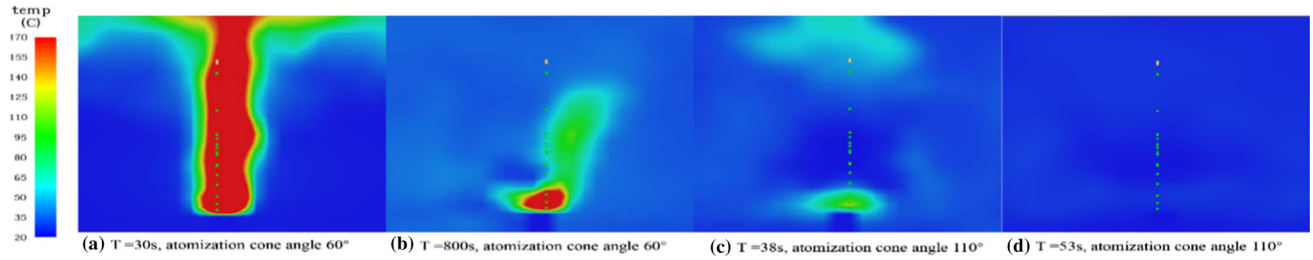

Fig. 9 Contour map of x = 0.1 plane temperature at different times

Table 7 Extinguishing time under the conditions of different spray speeds

Spray speed ($m \cdot s^{-1}$)	5	10	20	30
Time to reduce to safe temperature (s)	69	58	54	58
Time to room temperature (s)	81	64	62	65

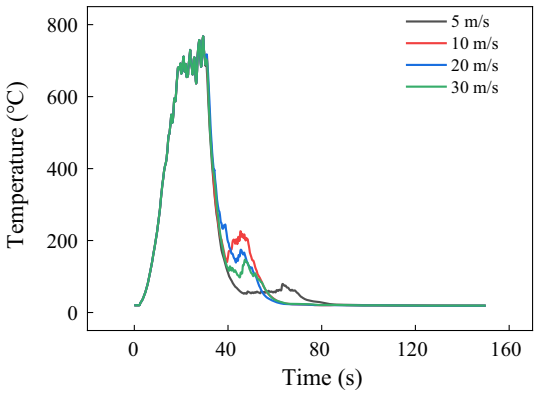

Fig. 10 The curve of fuel surface temperature

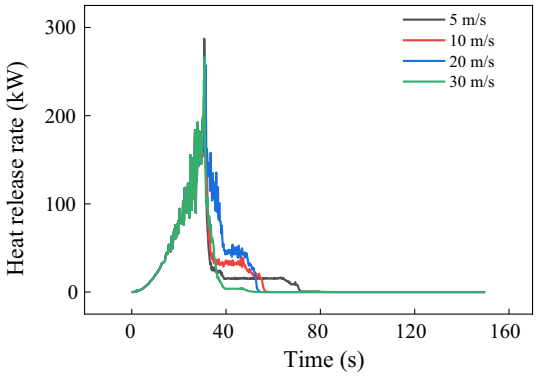

Fig. 11 The curve of heat release rate change

to a certain extent. However, when the spray speed continues to increase to 30 m/s, the fire suppression effect decreases slightly. This may be because the momentum of water mist increases with the increase of spray speed, so it is easier to reach the low-temperature area below the fire source in the fire site, which affects the evaporation and heat absorption process and reduces the cooling and fire extinguishing efficiency of water mist. So, the spray speed should not be too large. In similar scenarios, the spray speed that can greatly improve the cooling effect is 20 m/s. The spray speed has a significant effect on restraining heat release rate.

3.2.2 Analysis of Heat Release Rate and Thermal Radiation

Figures 11 and 12 show the effect of water mist spray speed on heat release rate and thermal radiation, respectively. It can be seen from Fig. 11 that after opening the water mist nozzle,

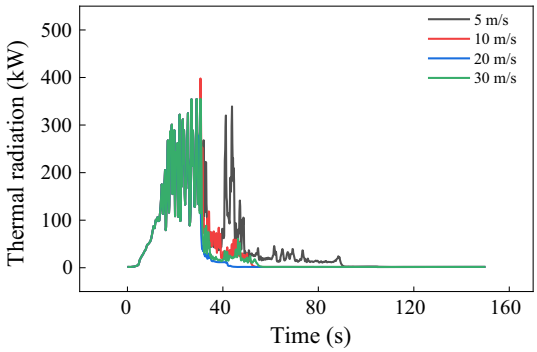

Fig. 12 The curve of thermal radiation change

when the spray speed is 5 m/s, the heat release rate drops to 0 kW at 72 s. When the spray speed is 10 m/s, the heat release rate drops to 0 kW at 56 s. When the spray speed is set to 20 m/s, the heat release rate drops to 0 kW at 54 s. When spray speed is 30 m/s, the heat release rate drops to 4 kW at 39 s.

It can be seen from Fig. 12 that when the spray speed is 5 m/s, the thermal radiation will still rise greatly after the nozzle is turned on, but the fluctuation time is relatively short, about 10 s. At 50 s, the thermal radiation has stabilized below 40 kW. When the spray speed increases, due to the increase of momentum, the direct suppression of fire source is enhanced, and the thermal radiation no longer rises greatly, which is significantly reduced to less than 40 kW within 50 s. The shielding effect of several groups of working conditions on thermal radiation is good, which shows that the spray speed has a low impact on thermal radiation.

3.3 Effect of Droplet Size on Fire Extinguishing

In order to explore the influence of droplet size on fire extinguishing effect in confined space in water mist device, four different spray droplet sizes of 100 μm, 200 μm, 300 μm and 600 μm are numerically simulated when other parameters remained unchanged. Table 8 shows the parameter settings of water mist nozzle.

3.3.1 Oil Surface Temperature Analysis

The temperature of the fuel surface temperature measured with the four conditions is simulated with time. The cooling effect of the water mist fire extinguishing system is obtained

Table 8 Parameter setting of water mist nozzle

Water mist droplet size (μm)	Jet speed ($m \cdot s^{-1}$)	Flow ($L \cdot min^{-1}$)	Atomization cone angle (°)
100	20	10	110
200	20	10	110
300	20	10	110
600	20	10	110

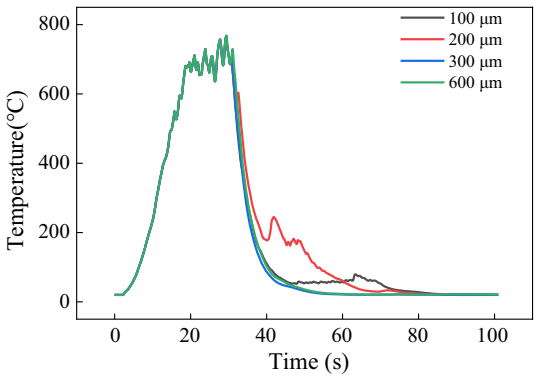

Fig. 13 The curve of temperature change

when the spray droplet size is different, as shown in Fig. 13 and Table 9. It can be seen that the moderate improvement of droplet size can increase the momentum, make the droplets contact the fuel directly faster, suppress the combustion, cool down quickly and significantly improve the fire extinguishing efficiency. However, when the droplet size is too large, it is not conducive to droplet evaporation, which affects the cooling process of water mist. Therefore, the droplet size of water mist should not be too large. In similar scenes, the droplet size that can improve the cooling effect most is 300 μm.

3.3.2 Analysis of Heat Release Rate and Thermal Radiation

Figures 14 and 15 show the effect of water mist droplet size on heat release rate and thermal radiation, respectively. It can be seen from Fig. 14 that the inhibition of water mist on heat release rate increases with the increase of droplet size. When the droplet size is 100 μm, the heat release rate decreases rapidly after the release of water mist, becomes stable at 40 s, continues to decline slowly at 70 s and finally decreases to 0 kW at 130 s. When the droplet size is 200 μm,

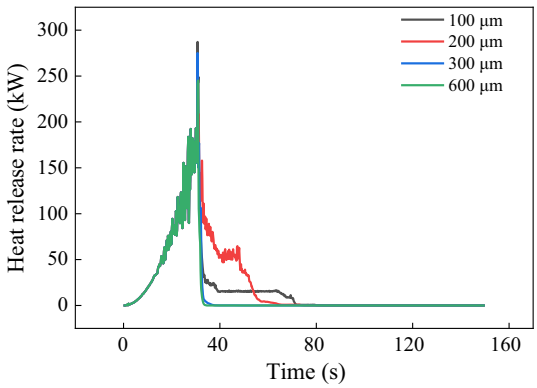

Fig. 14 The curve of heat release rate change

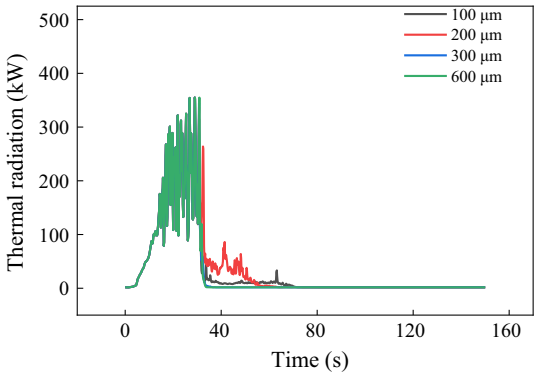

Fig. 15 The curve of thermal radiation change

the reduction rate of heat release rate with the droplet size of 200 μm is significantly lower than that of with the droplet size of 100 μm in the first 10 s. The decrease of heat release rate accelerates at 50 s and finally decreases to 0 kW at 105 s. This is because the temperature at the initial stage of water mist release is higher, and the water mist with small particle size has a larger relative surface area and is easier to be heated and evaporated. The fire suppression effect of 100 μm is obviously better than that of 200 μm. As the temperature of the fire site decreases, the evaporation efficiency of droplets also decreases compared with that of the high-temperature fire site. Large particle size droplets are easier to fall to the fuel surface and directly inhibit the fuel combustion. When the droplet size is 300 μm, the droplet momentum also continues to increase, and it can easily pass through the fire site and fall near the fuel. Therefore, the fire suppression effect is still improving, and the heat release rate is no longer in

Table 9 Extinguishing time under different spray droplet size conditions

Droplet size (μm)	100	200	300	600
Time to reduce to safe temperature (s)	69	60	42	44
Time to room temperature (s)	81	76	52	56

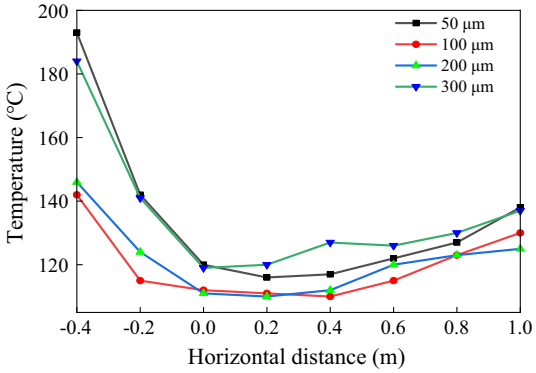

Figure16 Horizontal distribution of temperature at 0.1 m below the ceiling

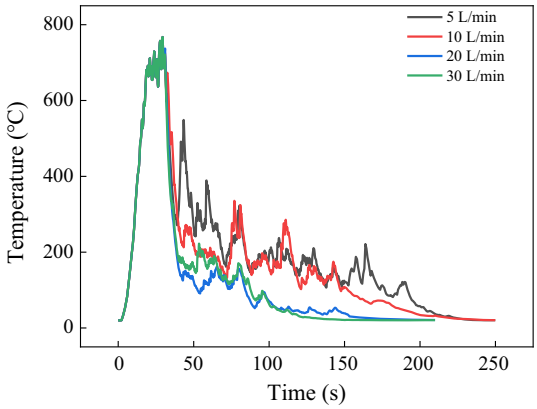

Fig. 17 The curve of temperature change

a plateau period. At 71 s, the heat release rate decreases to 0 kW. When the droplet size is 600 μm, the reduction rate of heat release rate is unstable, and it fluctuates repeatedly until 82 s. Compared with the working condition of 300 μm, the inhibition effect on the heat release rate with droplet size of 600 μm has not increased significantly. To sum up, water mist with droplet size of 300 μm has the best inhibition effect on the heat release rate of fire source.

It can be seen from Fig. 15 that when the droplet size of water mist is 100 μm, the thermal radiation of the fire site decreases significantly and is close to 0 kW at 70 s. When the droplet size is 200 μm, the thermal radiation is close to 0 kW at 62 s. This is because the fire site temperature is high from 30 to 50 s, which is conducive to the evaporation of small droplet size water mist, the thermal radiation shielding effect of fine water mist with the droplet size of 100 μm is better, but the smoke temperature decreases in the later stage, and the advantage of small droplet size water mist is no longer. The momentum of slightly larger droplet size water mist is enough to suppress the fire faster. Under the working condition with larger droplet size of 300 μm, the smoke can penetrate the fire source earlier, so the effect of shielding thermal radiation is also better, thermal radiation change curve of water mist with the droplet size of 600 μm is very close to that with the droplet size of 300 μm, and the lifting effect is not obvious. In general, the inhibition effect is obvious in several groups of working conditions with different droplet sizes, but water mist with the droplet size of 300 μm has the fastest suppression rate of thermal radiation.

Figure 16 shows the horizontal distribution of hot flue gas temperature at 0.1 m below the ceiling after applying water mist with different droplet sizes in the fire room for 30 s. It can be seen that the farther away from the fire source, the better the cooling effect of small-diameter water mist is, and the cooling condition is stronger than that of large-diameter droplets. This is because water mist with the droplet size of less than 100 μm has a certain fluidity. The droplets can follow the airflow in the room to disperse to the range outside the spray cone angle to play a cooling role. Therefore, when the water mist cannot be directly sprayed into the fire site with obstacles, the dispersion of small particle droplets will help to cool the ambient temperature at the fire site and improve the fire extinguishing efficiency.

Table 10 Parameter settings of water mist nozzle

Water mist droplet size (μm)	Jet speed ($m \cdot s^{-1}$)	Flow ($L \cdot min^{-1}$)	Atomization cone angle (°)
300	20	5	110
300	20	10	110
300	20	20	110
300	20	30	110

3.4 Effect of Spray Flow on Fire Suppression

3.4.1 Analysis of Oil Surface Temperature

In order to investigate the influence of droplet size in water mist devices on fire extinguishing effect in confined space, four different spray flows of 5 L/min, 10 L/min, 20 L/min and 30 L/min are selected for numerical simulation when other parameters remain unchanged. When the spray flow is different, the spray cooling effect of pulse water mist fire extinguishing system is shown in Fig. 17, and Table 10 is the parameter settings of water mist nozzle. Table 11 shows extinguishing time under the conditions of different spray flows.

It can be seen from Fig. 17 that after 30 s of pre-combustion, the maximum temperature at the measuring point reaches 762 °C, and the fire extinguishing scenarios under the conditions of four spray flows can be successfully

Table 11 Extinguishing time under the conditions of different spray flows

Spray flow ($L \cdot min^{-1}$)	5	10	20	30
Time to reduce to safe temperature (s)	202	180	102	101
Time to room temperature (s)	225	221	160	148

extinguished, but the difference in fire extinguishing time is obvious. At 30 s, the temperature drops rapidly after the water mist nozzle is opened, and the working condition with the spray flow of 5 L/min drops to the safe temperature and does not rise at 202 s. When the spray flow increases to 10 L/min, the temperature decreases more rapidly. At 180 s, the temperature is safe, but the time to recover to room temperature is not different from that of 5 L/min. The overall temperature change trend is similar to that of 5 L/min. The temperature rise amplitude decreases, and the maximum temperature is only 335 °C, which is 38% lower than the maximum temperature under the working condition of 5 L/min. The fire site temperature is restrained to a certain extent with the increase of water mist flow.

When the water mist flow increases again, the fire site temperature suppression effect is more obvious. After the water mist is turned on, it decreases rapidly to about 150 °C and continues to float slightly without obvious recovery. It decreases to the safe temperature at 102 s and extinguishes the fire successfully. When the flow increases to 30 L/min again, the overall trend of temperature change is similar to that of 20 L/min, but the time to reduce to the safe temperature is 101 s, which is not significantly reduced, compared with the working condition of 20 L/min. The time to recover to room temperature with the spray flow of 30 L/min is 12 s shorter than that with the spray flow of 20 L/min.

To sum up, after the flow increases to 20 L/min, the inhibition effect on the fire site temperature is very significant. Under the working condition of 30 L/min, the temperature can be reduced to 60 °C at about 100 s and will not rise again. The fire has been effectively controlled. Therefore, when the flow increases again, the optimization effect is relatively small and the fire extinguishing time will not be significantly reduced.

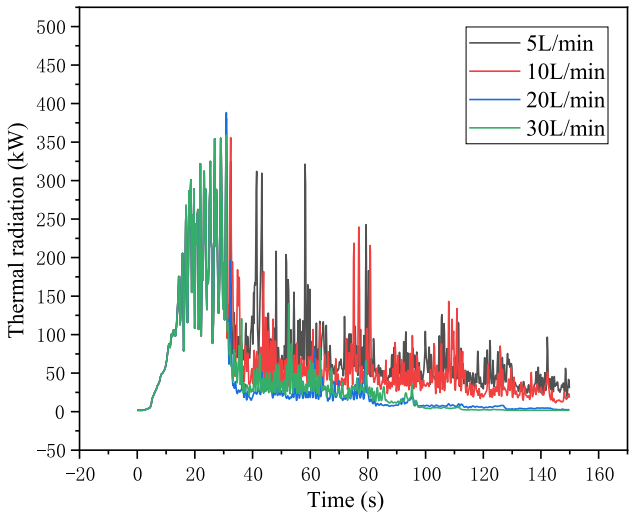

Fig. 18 The curve of heat release rate change

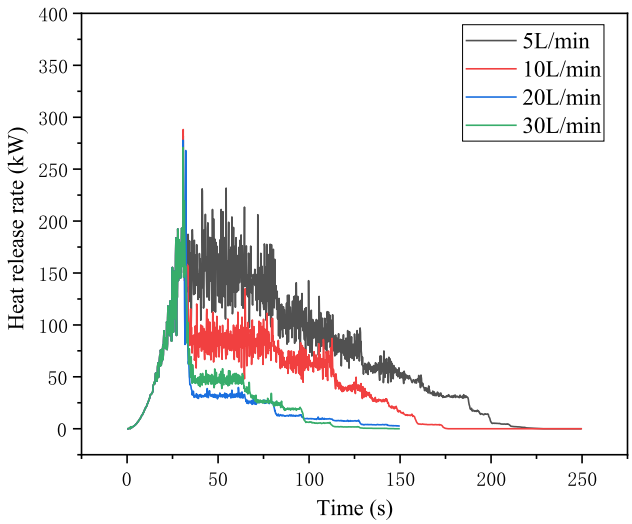

Fig. 19 The curve of thermal radiation change

3.4.2 Analysis of Heat Release Rate and Thermal Radiation

Figures 18 and 19 show the effect of spray flow on heat release rate and thermal radiation, respectively. It can be seen from Fig. 18 that when the spray flow is 5 L/min, the heat release rate in the confined space rapidly decreases to 180 kW after the nozzle is turned on, and then decreases in steps after 82 s, and effectively decreases to 60 kW at 130 s with small fluctuations. When the water mist spray flow is 10 L/min, the heat release rate decreases faster and decreases to 17 kW at 150 s. When the spray flow is 20 L/min, the heat release rate decreases to 0 kW at 140 s after the nozzle is turned on. When the spray flow is 30 L/min, the attenuation effect of heat release rate has little difference compared with the previous group of working conditions. After the nozzle is turned on, the heat release rate drops to 0 kW at 130 s. It can be seen from Fig. 19 that when the spray flow is 5 L/min, the thermal radiation fluctuates greatly after the water mist system is started. When the spray flow is 10 L/min, the overall variation amplitude of 10 L/min is similar to that of 5 L/min,

but the fluctuation amplitude and peak value of 10 L/min are reduced, and the shielding effect on thermal radiation of 10 L/min is obviously better than that of 5 L/min. The change of thermal radiation of 20 L/min is similar to that of 30 L/min. The effect of thermal radiation suppression for water mist with the spray flow of 20 L/min is the most stable in the scene. When the spray flow is greater than 20 L/min, the fire extinguishing effect is weak, so the water mist spray flow of 10–20 L/min is more appropriate.

4 Conclusions

Large eddy method and Lagrange method are used to simulate the process of water mist and pool fire in confined space. By changing the spray cone angle, spray speed, droplet size and spray flow, the effects of water mist on the temperature, heat release rate and thermal radiation in confined space are investigated, and the mechanism of water mist fire extinguishing is deepened. The conclusions can be drawn as follows.

1) The atomization cone angle affects the spray arrangement of water mist and the contact area of high-temperature flue gas. The atomization cone angle is 80°–110°, and the fire extinguishing time is gradually shortened. The cooling effect of water mist is improved with the increase of atomization cone angle. When the atomization cone angle is greater than 110°, the fire extinguishing time is no longer significantly shortened. With the increase of atomization cone angle, the inhibition effect of water mist on heat release rate increases. When the atomization cone angle is 50°–120°, the atomization cone angle with the best cooling effect is 110°.
2) The relationship between spray speed and fire extinguishing capacity is nonlinear. When the spray speed is 5–20 m/s, the greater the spray speed, the better the cooling and fire extinguishing effect. When the spray speed is 30 m/s, the fire suppression effect decreases. Spray speed has little effect on thermal radiation, but has a significant effect on restraining heat release rate.
3) When the droplet size is 100–300 μm, the larger the droplet size is, the faster the cooling rate of the fire is, and the fire extinguishing effect is remarkable. When the droplet size is greater than 300 μm, the relative specific surface area of droplets decreases, which inhibits the cooling rate of the fire site. The inhibition of water mist on heat release rate increases with the increase of droplet size. The water mist with small particle size has a better cooling effect on the ceiling because of its overflow effect. In a naturally ventilated room, the water mist with small diameter is easy to disperse; the particle with a larger momentum of 300 μm has a good effect on oil surface temperature reduction.
4) The increase of spray flow can significantly improve the fire extinguishing performance of water mist and effectively control the fire. When the spray flow is greater than 20 L/min, the fire extinguishing effect is weak, and the water mist spray flow of 10–20 L/min is more appropriate.

Acknowledgements The authors acknowledge the financial support provided by the Fundamental Research Funds for the Central Universities (Grant No. 2021YJSAQ19) and Yueqi Scholar Program for China University of Mining and Technology (Beijing).

Declarations

Conflict of interest The authors declare that they have no known competing financial interests or personal relationships that could have appeared to influence the work reported in this paper.

References

1. Yang, X.; Liu, D.; Yao, B.: Reliability analysis of restrained steel beam in natural fire. Engineering Journal of Wuhan University, China (2012)
2. Gupta, M.; Pasi, A.: An experimental study of the effects of water mist characteristics on pool fire suppression. Exper Therm Fluid Sci **44**, 768–778 (2013)
3. Yang, L.; Zhao, J.: Fire extinct experiments with water mist by adding additives. J. Therm. Sci. **20**, 563–569 (2011)
4. Santangelo, P.E.; Jacobs, B.C.; Ren, N.; Sheffel, J.A.; Corn, M.L.; Marshall, A.W., et al.: Suppression effectiveness of water-mist sprays on accelerated wood-crib fires–Science Direct. Fire Safety J **70**, 98–111 (2014)
5. Arvidson, M.: Large-scale water spray and water mist fire suppression system tests for the protection of ro ro cargo decks on ships. Fire Tech. **50**, 589–610 (2014)
6. Chiu, C.W.; Li, Y.H.: Full-scale experimental and numerical analysis of water mist system for sheltered fire sources in wind generator compartment. Process Saf. Environ. Prot. **98**, 40–49 (2015)
7. Schmidt, M.M.; Nielsen, L.H.; Søgaard, S.V.: Study of water-mist behaviour in hot air induced by a room fire: model development, validation and verification. J. Ethnopharmacol. **168**, 380 (2015)
8. Vouros, A.; Vouros, A.; Panidis, T.: Experimental study of a water-mist jet issuing normal to a heated flat plate[J]. Therm Sci J **20**, 473–482 (2016)
9. Santangelo, P.E.; Tartarini, P.; Tarozzi, L.: Full-scale experiments of fire control and suppression in enclosed car parks: a comparison between sprinkler and water-mist systems. Fire Technol. **52**, 1369–1407 (2016)
10. Wang, L.; Su, S.C.; Wei, C.Y.: A study on the flow field and the structure of fire plumes in the coupling process of the water mist and the jet fire of diesel fuel. Procedia Eng **211**, 736–746 (2018)
11. You-Wei, D.U.; Guo, Y.; Cao, A.X.: Design of direct-swirl premixed water mist nozzle and experimental study on oil-fire extinguishing[J]. Fire Sci Tech **38**, 827–832 (2019)
12. Liu, W.Y.; Chen, C.H.; Shu, Y.L.; Chen, W.T.; Shu, C.M.: Fire suppression performance of water mist under diverse desmoking and ventilation conditions. Process Saf Environ Protect **133**, 230–242 (2020)

13. Lin, Y.J.; Hu, L.H.; Zhang, X.L.; Chen, Y.H.: Experimental study of pool fire behaviors with nearby inclined surface under cross flow. Process Saf. Environ. Prot. **148**, 142–150 (2021)
14. Zhao, J.C.; Lu, S.; Fu, Y.Y.; Shahid, M.U.; Zhang, H.: Application of ultra-fine dry chemicals modified by POTS/OBS for suppressing aviation kerosene pool fire. Fire Saf J (2020). https://doi.org/10.1016/j.firesaf.2020.103148
15. Wu, C.; Zhou, T.; Chen, B.: Experimental study on burning characteristics of the large-scale transformer oil pool fire with different extinguishing methods. Fire Technol. **57**, 46–52 (2020)
16. Ji, J.; Ge, F.L.; Qiu, T.T. 2020 Experimental and theoretical research on flame emissivity and radiative heat flux from heptane pool fires. Proceedings of the Combustion Institute. **45**, 47
17. Tian, X.L.; Liu, C.; Zhong, M.H.; Shi, C.L.: Experimental study and theoretical analysis on influencing factors of burning rate of methanol pool fire. Fuel **269**, 99–107 (2020)
18. Chen, Z.; Wei, X.L.; Li, Ten: experimental investigation on flame characterization and temperature profile of single/multiple pool fire in cross wind. J Therm Sci. **30**, 69–73 (2020)
19. Kong, D.P.; Yang, H.B.; He, Xu.: Impact of wind on in-situ burning behavior of spilled oil on open water. J. Loss Prev. Process Ind. **65**, 21–27 (2020)
20. Gelderen, L.V.; Alva, U.R.; Mindykowski, P.: Thermal properties and burning efficiencies of crude oils and refined. Int Oil Spill Conf (2017). https://doi.org/10.7901/2169-3358-2017.1.985
21. Joe, H.S.; Choi, C.S.: A study on combustion patterns of flammable liquids by contained oil test. Fire Sci Eng. **28**, 14–20 (2014)
22. Mcgrattan, K.: Fire Dynamics simulator, User's Guide[M]. Nist special publication (2013)
23. Clayton, H.: Combustion conditions and exposure conditions for combustion product toxicity testing. J. Fire Sci. **2**, 328–347 (2015)